Structure and mechanism of β-hairpin antimicrobial peptides in lipid bilayers from solid-state NMR spectroscopy

Ming Tang and Mei Hong*

Received 14th November 2008
First published as an Advance Article on the web 27th January 2009
DOI: 10.1039/b820398a

The membrane-bound structure, lipid interaction, and dynamics of the arginine-rich β-hairpin antimicrobial peptide PG-1 as studied by solid-state NMR are highlighted here. A variety of solid-state NMR techniques, including paramagnetic relaxation enhancement, ^{1}H and ^{19}F spin diffusion, dipolar recoupling distance experiments, and 2D anisotropic–isotropic correlation experiments, are used to elucidate the structural basis for the membrane disruptive activity of this representative β-hairpin antimicrobial peptide. We found that PG-1 structure is membrane dependent: in bacteria-mimetic anionic lipid membranes the peptide forms oligomeric transmembrane β-barrels, whereas in cholesterol-rich membranes mimicking eukaryotic cells the peptide forms β-sheet aggregates on the surface of the bilayer. PG-1 causes toroidal pore defects in the anionic membrane, suggesting that the cationic arginine residues drag the lipid phosphate groups along as the peptide inserts. Mutation of PG-1 to reduce the number of cationic residues or to change the arginine guanidinium structure significantly changes the degree of insertion and orientation of the peptide in the lipid membrane, resulting in much weaker antimicrobial activities.

Antimicrobial peptides

Antimicrobial peptides (AMPs) are small cationic peptides produced by the innate immune system of many animals and plants to kill a broad spectrum of microbes, including bacteria, fungi, and viruses.[1] AMPs have a diverse range of secondary structures. For instance, magainin from the African clawed frog[2] and LL-37 from human[3] are α-helical peptides. Tachyplesins from the horseshoe crab[4] and protegrins from porcine leukocytes[5] are antiparallel β-hairpin peptides constrained by multiple disulfide bonds. Aromatic-rich peptides such as indolicidins and tritrpticin adopt turn-rich structures.[6] Despite this structural diversity, most AMPs share the common feature that their cationic residues are spatially well separated from the hydrophobic residues, thus making the overall structure of these molecules amphipathic. AMPs distinguish the microbial cells from eukaryotic cells by taking advantage of the difference that microbial cell membranes have a significant percentage of anionic phospholipids and no cholesterol, while eukaryotic cell membranes contain

Department of Chemistry, Iowa State University, Ames, IA 50011, USA. E-mail: mhong@iastate.edu; Fax: +1 515 294 0105; Tel: +1 515 294 3521

Ming Tang

Dr Ming Tang received his PhD in Chemistry from Professor Mei Hong's group at Iowa State University in 2008. His research has focused on solid-state NMR investigations of the structure and dynamics of β-hairpin antimicrobial peptides in lipid membranes. He is now a postdoctoral research associate in Professor Chad Rienstra's group at the University of Illinois at Urbana-Champaign. His current research interest is the structure of membrane proteins involved in disulfide bond formation.

Mei Hong

Dr Mei Hong, John D. Corbett Professor of Chemistry at Iowa State University, received her BA degree from Mount Holyoke College in 1992 and her PhD from the University of California at Berkeley in 1996. Following one year of research at the Massachusetts Institute of Technology as an NIH postdoctoral fellow and two years at the University of Massachusetts at Amherst as a research professor, she joined the faculty at Iowa State University in 1999. Her research focuses on the development and application of solid-state NMR techniques to investigate the structure and dynamics of membrane peptides and proteins, fibrous proteins, and complex biopolymers.

This journal is © The Royal Society of Chemistry 2009

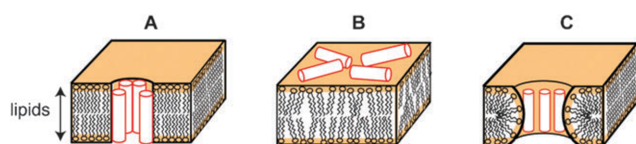

Fig. 1 Three models of membrane disruption by antimicrobial peptides. (A) Barrel-stave model. (B) Carpet model. (C) Toroidal pore model.

mostly zwitterionic phospholipids and a high level of cholesterol.[7] These fundamental differences are particularly pronounced in the outer leaflet of the cell membrane, with which the peptides interact upon first contact.[8,9]

While it is generally agreed that membrane disruption is the main *modus operandi* of AMPs, distinct peptide–lipid interactions have been observed for various AMPs, leading to three main models of antimicrobial mechanism. In the "barrel-stave" model (Fig. 1A), the peptides aggregate into transmembrane (TM) helical bundles that insert into the bilayer to form pores, which subsequently lyse the cell. This model was used to explain the step-wise conductivity increases in alamethicin-containing membranes.[10,11] In the "carpet" model (Fig. 1B), the peptides accumulate on the bilayer surface with the hydrophobic face embedded shallowly in the hydrophobic region of the membrane, while the positive charges are directed toward the hydrophilic water. When the peptide concentration exceeds a threshold, the bilayers are disrupted into micelles, thus killing the cell. This model was initially proposed based on studies of dermaseptin.[12] In the toroidal pore model (Fig. 1C), the aggregating peptides cause lipid disorder such that the two leaflets of the bilayer merge to form a torus-shaped pore. This model was proposed to explain the large water-filled cavities[13] and increased lipid flip-flop rate[14] caused by magainin.

Protegrin-1 (PG-1) is one of a family of peptides isolated from porcine leukocytes.[15] It possesses broad-spectrum activity against Gram-positive and Gram-negative bacteria, fungi, and some enveloped viruses.[5] Its minimum inhibitory concentrations are a few micrograms per millilitre.[16] PG-1 has eighteen amino acids, six of which are arginines (Arg) (Fig. 2A). Two disulfide bonds constrain the molecule to a β-hairpin fold, with the β-strand region containing residues 4–8 and 13–17 and the β-turn containing residues 9–12. PG-1's secondary structure is representative of many β-hairpin AMPs; thus the peptide is a good model system for understanding the interaction of this class of AMPs with lipid membranes. An extensive structure–activity relationship (SAR) study has been conducted on several hundred protegrin analogues.[17] It was found that the overall amphiphilicity, charge density, intermolecular hydrogen-bonding capability, and the hairpin fold are more important to activity than the presence of specific amino acids and stereochemistry. Lipid vesicle leakage assays[18,19] and neutron diffraction of oriented lipid bilayers[20] indicated that PG-1 carries out its function by forming pores in the microbial cell membrane. However, the high-resolution structure of the peptide and its supramolecular assemblies at these pores were not known. Solid-state NMR (SSNMR) spectroscopy is an excellent technique to determine the atomic-resolution structure of membrane-bound peptides

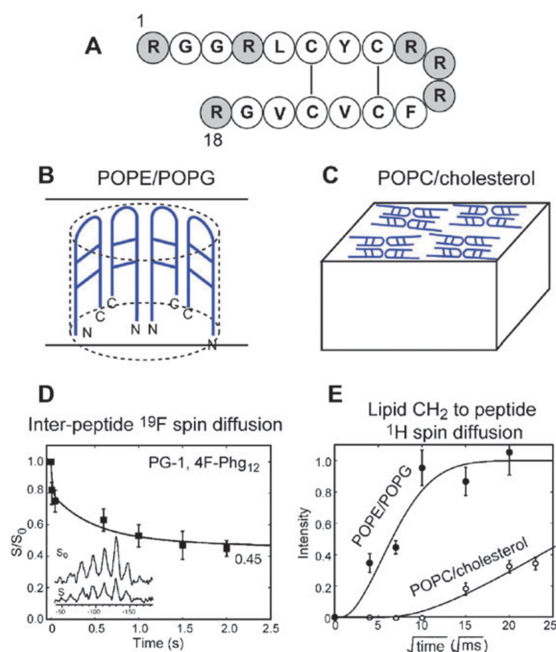

Fig. 2 (A) Amino acid sequence of PG-1 with the Arg residues shaded. (B) The depth of insertion, orientation, and oligomeric structure of PG-1 in anionic POPE–POPG membranes. (C) The depth of insertion and oligomeric structure of PG-1 in neutral POPC–cholesterol membranes. (D) Representative ^{19}F spin diffusion data that yielded the oligomeric structure of PG-1 in the lipid membrane.[29] (E) Representative lipid–protein ^{1}H spin diffusion data that yielded the transmembrane insertion of PG-1 in anionic membranes and surface-bound state in neutral cholesterol-containing membranes.[29]

and proteins.[21,22] We have conducted an extensive SSNMR study of the interaction of PG-1 with lipids and the topological structure of PG-1 in lipid membranes of different compositions, which reveal the origin of PG-1's antimicrobial activity.[23]

Depth and orientation of β-hairpin antimicrobial peptides in lipid membranes

The insertion and orientation of β-sheet membrane proteins in lipid bilayers have not been well studied compared to their α-helical counterparts. We demonstrated a method to determine the depths of insertion of membrane peptides that utilizes the paramagnetic relaxation enhancement (PRE) effect. Paramagnetic ions such as Mn^{2+} readily bind to the surface of lipid bilayers and enhance nuclear spin T_2 relaxation in a distance-dependent fashion.[24,25] The closer the nuclei are from the membrane surface, the faster the T_2 relaxation, and the lower the NMR intensity. Thus, intensity decreases of the protein compared to a control sample without the paramagnetic ions reflect the depths of individual residues from the bilayer surface. Further, one can calibrate the peptide depths by comparing with the lipid signals, since the depths of lipid segments are well known from X-ray and neutron diffraction data.[26] Applying this technique to PG-1 in DLPC bilayers, we found that residues at the N-terminus and the β-turn of the peptide experience strong PRE whereas residues in the middle of the

 This journal is © The Royal Society of Chemistry 2009

strands experience weaker PRE effects. Thus, the β-hairpin peptide is fully inserted across the lipid bilayer.[24]

The lipid-calibrated PRE technique is most applicable to mobile membrane peptides. To determine the depths of immobile molecules, which can be either large membrane proteins or highly oligomerized membrane peptides, ^{1}H spin diffusion from the lipids to the protein is a more suitable technique. In this experiment, the lipid chain protons transfer their magnetization to the protein in a distance-dependent fashion and are detected through the protein ^{13}C signals. The lipid–protein ^{1}H–^{13}C cross peak intensities depend on the depth of insertion of the protein. The intensity buildup as a function of the spin diffusion mixing time yields semi-quantitative distances (±2 Å) of the protein from the center of the bilayer.[27] Using this technique, we found that PG-1 is in close contact with the lipid methyl groups both in zwitterionic 1-palmitoyl-2-oleoyl-*sn*-glycero-3-phosphatidylcholine (POPC) membranes[28] and in mixed anionic membranes containing 1-palmitoyl-2-oleoyl-*sn*-glycero-3-phosphoethanolamine (POPE) and 1-palmitoyl-2-oleoyl-*sn*-glycero-3-phosphatidylglycerol (POPG)[29,30] (Fig. 2B, E). In contrast, PG-1 is ~20 Å from the hydrophobic center of POPC–cholesterol membranes, since the lipid chain–peptide cross peaks are very weak even at long mixing times (Fig. 2C, E). Thus, the membrane composition has a significant effect on PG-1 insertion: the bacteria-mimetic anionic membrane POPE–POPG allows PG-1 insertion, while the eukaryotic POPC–cholesterol membrane prevents PG-1 insertion.

Orientation information complements depth measurements in elucidating the topology of AMPs in lipid bilayers. The orientations of α-helical membrane proteins in lipid bilayers have been well studied using 2D separated-local field (SLF) NMR correlating the ^{15}N chemical shift anisotropy (CSA) with the ^{15}N–^{1}H dipolar coupling on macroscopically aligned samples.[31,32] This strategy is also applicable to β-sheet membrane proteins but with very different characteristic spectral patterns.[33–35] The reason is that the N–H bonds, which correspond to the main direction of the ^{15}N chemical shift tensor and the N–H dipolar tensor, are not along the main molecular axis, the β-strand axis, of β-sheet peptides. This makes the ^{15}N CSA and N–H dipolar tensors not very diagnostic of the β-strand orientation, unless a sufficient number of ^{15}N constraints are measured. In comparison, the ^{13}CO chemical shift tensor is ideally sensitive to the β-sheet geometry: its x principal axis points along the β-strand axis and its z principal axis points along the normal of the β-sheet plane. Thus, ^{13}CO CSA measurements on aligned β-sheet membrane peptides give relatively clear orientation information. We used both the 2D ^{15}N SLF technique and the 1D ^{13}CO CSA experiment to determine the orientations of several β-hairpin AMPs. For the cyclic β-hairpin AMP retrocyclin, the 2D ^{15}N SLF spectra indicated a TM orientation of the peptide in DLPC bilayers.[35] For PG-1, ^{13}CO and ^{15}N CSAs constrained the peptide to a tilted orientation in DLPC bilayers, with the strand axis ~55° from the bilayer normal.[36] For the horseshoe crab β-hairpin AMP tacheplesin-1 (TP-I), ^{13}CO and ^{15}N CSAs indicate an in-plane orientation, with an angle of ~20° between the β-sheet plane and the membrane surface.[37]

Since AMPs tend to disrupt lipid membranes, macroscopically aligned bilayers that underlie the above orientation-dependent spectra are often difficult if not impossible to prepare. Even when aligned, the membrane composition that allows the alignment may not be the most biological. To overcome this difficulty, we exploited the fact that many small membrane peptides undergo uniaxial rotation around the bilayer normal at rates faster than the CSA and dipolar interactions. Under this fast uniaxial rotation, it can be shown that the 0° (90°) frequency of the motionally averaged spectra of an unoriented sample is identical to the frequency of an oriented sample whose alignment axis is parallel (perpendicular) to the magnetic field.[37,38] Thus, if the peptide is uniaxially mobile, then one can avoid alignment altogether and use powder samples and magic-angle spinning (MAS) experiments to determine the peptide orientation. This approach was demonstrated on PG-1, TP-I, and an α-helical membrane peptide, the M2 peptide of influenza A virus.[37,38] The presence of fast uniaxial rotation can be verified from the powder patterns of CSA tensors that are large and non-uniaxial in the rigid limit.[39] If the powder patterns are not only narrowed from the rigid-limit value but also have an asymmetry parameter of 0, then it is a strong indication that the molecule undergoes fast uniaxial rotation.

Oligomeric structure of β-hairpin antimicrobial peptides

Most models of antimicrobial action invoke peptide oligomerization as a prerequisite for membrane disruption. SAR studies of PG-1 showed that linearized mutants and mutants that eliminate potential hydrogen bonds between β-hairpins have weaker activities.[17] A solution NMR study of PG-1 in dodecylphosphocholine micelles[40] showed ^{1}H–^{1}H NOE's indicative of antiparallel dimers where the C-terminal strand lines the dimer interface. But micelles tend to impose curvature strains onto peptides and may not reflect the oligomeric state of the peptide in lipid bilayers. We found that PG-1 backbone is immobilized in POPC bilayers in the liquid-crystalline phase, which is not possible if the peptide is monomeric.[28] Quantitative ^{19}F spin diffusion experiments (Fig. 2D) showed that PG-1 is indeed oligomerized in membranes with lipid chain lengths of 16–18.[41,42] In POPC and POPE–POPG bilayers, PG-1 assembles with the same strands lining the intermolecular interface and with each ^{19}F in a two-spin environment. Further, the β-hairpins in this ···NCCNNCCN··· assembly are parallel instead of antiparallel, based on intermolecular ^{1}H–^{13}C, ^{13}C–^{19}F, and ^{13}C–^{15}N distance experiments.[43] Since PG-1 is also transmembrane in the same bacteria-mimetic membranes based on ^{1}H spin diffusion experiments, and leakage assays indicate pores with a diameter of ~20 Å, we conclude that PG-1 oligomerizes into TM β-barrels of 8–10 molecules[29] (Fig. 2B). Interestingly, the peptide also forms structured aggregates similar to amyloid fibrils in the absence of lipid bilayers, and the intermolecular packing was found by 2D ^{13}C–^{13}C correlation experiments to be parallel with like strands at the interfaces.[44] Thus the fibrilized PG-1 structure is very similar to the membrane-bound structure. In the POPC–cholesterol membrane, ^{19}F

spin counting experiments revealed larger spin clusters of at least 4, indicating that the peptide aggregates more extensively. Moreover, lipid-to-peptide ^{1}H spin diffusion experiments revealed that PG-1 lies on the surface of the cholesterol-rich membrane. Thus, PG-1 assembles into extended β-sheets on the surface of eukaryotic cell membranes (Fig. 2C).

Guanidinium–phosphate complexation between antimicrobial peptides and lipids

Most AMPs are rich in Arg. However, the exact role of cationic residues in antimicrobial activities had not been elucidated with high-resolution structural input. SAR studies indicated that protegrin mutants with fewer Arg residues have weaker activities by as much as an order of magnitude compared to wild-type PG-1.[17] In general, the insertion of charged residues into the hydrophobic part of the lipid bilayer is energetically unfavorable. Measurement of the free energy[45,46] of transferring peptides from water to lipid bilayers using an endoplasmic reticulum translocon system gave positive free energies of about +2.5 kcal mol^{-1} for each Arg and Lys residue.[47] Despite this free energy cost, helical peptides containing multiple Arg residues have been found to insert into the lipid bilayer.[48] Molecular dynamics simulations suggested that Arg-rich peptides can insert into the membrane with the help of membrane thinning, the formation of Arg–water hydrogen bonds, and the formation of Arg–phosphate hydrogen bonds.[49,50]

The TM topology of PG-1 in non-cholesterol membranes would put some residues such as Arg_4 in the center of the bilayer, with apparently high free energy penalty. To understand how this occurs, we measured the ^{13}C–^{31}P distances between Arg residues and lipid phosphate groups. The TM topology predicts Arg's at the two ends of the molecule to be close to the ^{31}P while Arg_4 and other strand interior residues to be far from ^{31}P. Surprisingly, we found that Arg_4 has similarly short ^{13}C–^{31}P distances as Arg_{11} at the β-turn. All distances fall within 4.0 and 6.5 Å.[30] The shortest distance, 4.0 Å, is found between Arg_{11} Cζ and ^{31}P (Fig. 3C). Since Cζ is surrounded by NH groups while ^{31}P is surrounded by oxygen atoms, this short distance means that the guanidinium group must form hydrogen bonds with the PO_4 group (Fig. 3A). Further, ^{13}C–^{31}P distances for two consecutive residues along the β-strands indicate that the ^{31}P plane cannot be perpendicular to the TM hairpin but must be parallel to it. Thus, some lipid molecules must turn around to embed their headgroups into the hydrophobic region of the bilayer. This indicates toroidal pore defects created by PG-1 (Fig. 3B).

The driving force for this toroidal pore formation is most likely guanidinium–phosphate interactions. The guanidinium ion is responsible for most of Arg's non-covalent interactions and is known to form stable complexes with oxyanions such as phosphates, sulfates, and carboxylates.[51] The short distances between PG-1 Arg residues and lipid phosphates are thus not too surprising. The nature of this guanidinium–phosphate interaction is partly electrostatic, since the ^{13}C–^{31}P distances are ~2.0 Å longer in zwitterionic POPC membranes than in anionic POPE–POPG membranes.[44] The electrostatic nature is also supported by the findings that when the number of Arg

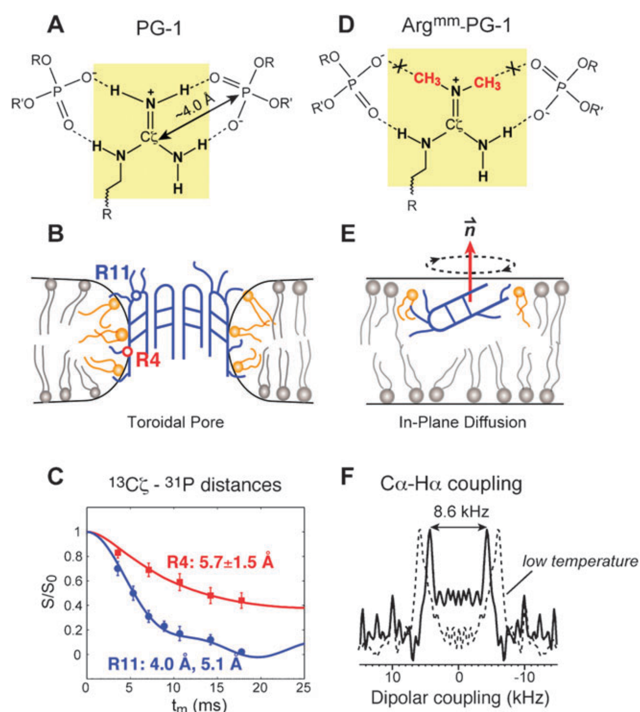

Fig. 3 (A) Guanidinium–phosphate complexes between PG-1 Arg residues and the lipid headgroups. (B) Toroidal pore model of PG-1 in anionic lipid membranes. For clarity, only half of the PG-1 β-barrel is shown. (C) Representative ^{13}C–^{31}P distance data of PG-1 that yielded the toroidal pore model.[30] (D) A dimethylated guanidinium group removes two potential hydrogen bonds with the lipid phosphates. (E) The orientation and depth of insertion of Arg^{mm}-PG-1 in the anionic membrane.[39] (F) Representative C–H dipolar coupling data that showed the dynamic structure and orientation of Arg^{mm}-PG-1.

residues was reduced from six to three, the mutant PG-1 inserted less deeply into the membrane and exhibited longer distances to ^{31}P (7.0–9.5 Å).[52] In zwitterionic POPC membranes, the Arg-reduced mutant is completely on the membrane surface, while in the 25% anionic POPC–POPG membranes, the mutant peptide is still about 8 Å from the membrane center.

The second factor stabilizing the guanidinium–phosphate complex is N–H···O=P hydrogen bonding. This is shown by an experiment where all Arg residues in PG-1 were mutated to dimethylated Arg (Fig. 3D), thereby removing two potential hydrogen bond donors per guanidinium ion. This Arg^{mm}-PG-1 peptide showed a three-fold reduction of antimicrobial activity, less membrane disorder as judged by ^{31}P NMR lineshapes, and longer peptide–lipid ^{13}C–^{31}P distances. Arg^{mm}-PG-1 is also highly dynamic,[39] suggesting that it is monomeric in the membrane, in contrast to the immobilized and oligomerized wild-type PG-1. The dynamics is uniaxial and is present at multiple backbone sites, thus it is likely whole-body rotational diffusion around the bilayer normal. We thus determined the orientation of Arg^{mm}-PG-1 by measuring motionally averaged Cα–Hα dipolar couplings of two strand residues (Fig. 3F) using unoriented MAS samples. Analysis of the orientation-dependent backbone bond order parameters indicates that the strand axis is tilted by 120° from the bilayer normal and the β-sheet plane is parallel to the bilayer normal[39] (Fig. 3E). Thus Arg^{mm}-PG-1 dips into the

This journal is © The Royal Society of Chemistry 2009

bilayer with its β-sheet plane meeting the least resistance, and this insertion mode is completely different from the wild-type peptide. It is striking that the removal of a few hydrogen-bonding groups in the guanidinium ions leads to such a significant change in the activity and structure of the peptide in the membrane. The remaining antimicrobial activity of Arg^{mm}-PG-1 is clearly mediated by a different mechanism, which we call in-plane diffusion.[53]

Dynamics of β-hairpin antimicrobial peptides in lipid membranes

Biological membranes are highly dynamic entities, with lipid molecules undergoing fast lateral diffusion and uniaxial rotational diffusion. As a result membrane proteins are also dynamic. Small membrane peptides often exhibit whole-body motion[54,55] while larger membrane proteins usually have significant segmental motions.[56,57] For AMPs, the dynamics is indicative of their oligomeric state and their interaction with the lipids. In particular, the motion of the Arg residues in AMPs is interesting to examine.

We compared the internal dynamics of two Arg residues in PG-1, one on the β-strand and the other at the β-turn. We measured dipolar couplings, CSAs, and relaxation times of these two residues in POPE–POPG-bound peptide.[58] The order parameters obtained from dipolar couplings (Fig. 4B) and CSAs showed that the backbone of Arg_4 on the β-strand is rigid, consistent with the highly oligomerized nature of the peptide in this membrane, whereas the backbone of Arg_{11} at the β-turn is mobile (Fig. 4A). This mobility is understandable because the β-turn is less involved in oligomerization and is close to the mobile water molecules on the membrane surface. Both Arg residues have highly mobile sidechains, but the Arg_4 sidechain has larger order parameters, or smaller amplitudes of motion, than Arg_{11}. This is also consistent with the fact that Arg_4 in the β-strand is heavily constrained by β-sheet packing.

For comparison, the mutant Arg^{mm}-PG-1 exhibits whole-body uniaxial rotation in the anionic lipid membrane, as indicated by reduced order parameters for the backbone of strand residues and uniaxial lineshapes of the Cα CSAs.[39] This supports a monomeric state of Arg^{mm}-PG-1 near the membrane surface. Thus, peptide dynamics clearly reflects the different interactions of PG-1 and Arg^{mm}-PG-1 with the lipid bilayer.

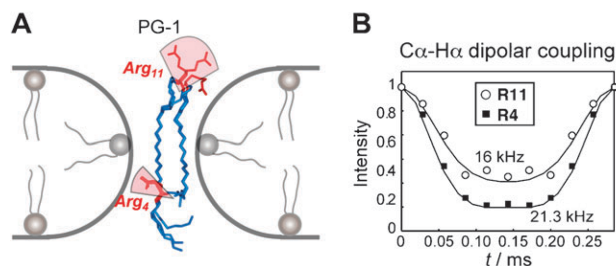

Fig. 4 (A) Dynamics of PG-1 arginine residues in the lipid membrane. Arg_{11} on the β-turn is much more mobile than Arg_4 on the β-strand. For simplicity, only two peptides are shown, although PG-1 is oligomerized into larger barrels. (B) Representative C–H dipolar coupling data that revealed the Arg dynamics in PG-1 in lipid membranes.[58]

Mechanism of antimicrobial activity of PG-1

Based on the above findings about PG-1 depth of insertion, orientation, oligomeric structure, dynamics, and interactions with the lipids, we conclude that a toroidal pore mechanism accounts for PG-1's antimicrobial activity (Fig. 3B). PG-1 molecules aggregate through intermolecular hydrogen bonds between β-strands and insert into the bilayers to form TM β-barrels that act as pores.[29] Due to the strong guanidinium–phosphate interaction, some lipid molecules are dragged by the Arg residues into the center of the bilayer, thus creating torus-shaped defects.[30] Because of the oligomerization and the TM orientation, the β-strands are close to the center of the bilayer and mostly rigid, while the β-turn is close to the membrane surface and is mobile. In contrast, the hydrogen-bond deficient Arg^{mm}-PG-1 resides on the membrane surface and undergoes fast uniaxial rotation around the bilayer normal in a monomeric state.[39] Despite the weaker interaction with the lipid headgroups, Arg^{mm}-PG-1, through its large-amplitude rotational diffusion in the plane of the membrane, disrupts the cell membrane (Fig. 3E). This in-plane diffusion mechanism also accounts for the activity of TP-I.[53]

Future outlook

The above review illustrates the rich structural and dynamical information that can be obtained from solid-state NMR studies of antimicrobial peptides and other membrane-active peptides. By examining three major structural aspects: orientation and insertion, lipid interaction, and oligomeric structure, one is well positioned to deduce the mechanism of action of these immune-defense molecules (Fig. 5). Peptide dynamics can affect the spectra of all three aspects and always needs to be examined in detail before the mechanism of action can be concluded.

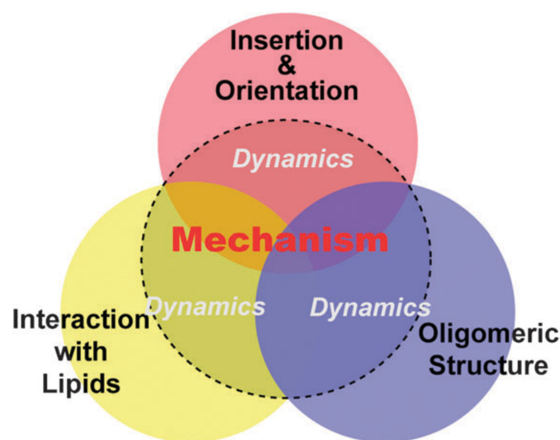

Fig. 5 Summary of the main structural aspects of antimicrobial peptides that have been studied using solid-state NMR. Insertion and orientation, interactions with lipids, and oligomeric structure information are combined to deduce the mechanism of action of the peptides. The peptide dynamics reflect all three aspects and is important to examine to validate the mechanism.

Future studies should investigate how general the above mechanism of action of PG-1 is among β-sheet antimicrobial peptides. Addressing this question will require comparative high-resolution structural studies of other peptides. Work from our laboratories suggests that changes in the distribution of the cationic residues *versus* hydrophobic residues can readily alter the antimicrobial mechanism, and formation of long-lasting pore is not the only mode of membrane disruption. Other mechanisms include, for example, membrane perturbation caused by highly dynamic peptides that undergo fast rotational diffusion in the membrane plane[39,53,55] and massive aggregation of peptides on the membrane surface.[52,53]

One family of β-sheet-rich antimicrobial peptides that is particularly worthy of SSNMR structural investigation is the human defensins.[59] These are larger peptides with more complex three-dimensional folds, as they contain not only β-strand segments but also coils and helices. Their direct relevance to human innate immune defense makes them important targets for high-resolution structure determination in the bilayer milieu.

Acknowledgements

This work is funded by NIH grant GM066976 to M. H.

References

1 R. M. Epand and H. J. Vogel, *Biochim. Biophys. Acta*, 1999, **1462**, 11–28.
2 M. Zasloff, *Proc. Natl. Acad. Sci. U. S. A.*, 1987, **84**, 5449–5453.
3 G. H. Gudmundsson, B. Agerberth, J. Odeberg, T. Bergman, B. Olsson and R. Salcedo, *Eur. J. Biochem.*, 1996, **238**, 325–332.
4 T. Nakamura, H. Furunaka, T. Miyata, F. Tokunaga, T. Muta, S. Iwanaga, M. Niwa, T. Takao and Y. Shimonishi, *J. Biol. Chem.*, 1988, **263**, 16709–16713.
5 L. Bellm, R. I. Lehrer and T. Ganz, *Expert Opin. Invest. Drugs*, 2000, **9**, 1731–1742.
6 D. I. Chan, E. J. Prenner and H. J. Vogel, *Biochim. Biophys. Acta*, 2006, **1758**, 1184–1202.
7 G. Rouser, G. J. Nelson, S. Fleischer and G. Simon, in *Biological Membranes; Physical Fact and Function*, ed. D. Chapman, Academic Press, London, New York, 1968, vol. 1, 5–69.
8 K. Matsuzaki, *Biochim. Biophys. Acta*, 1999, **1462**, 1–10.
9 Y. Shai, *Biochim. Biophys. Acta*, 1999, **1462**, 55–70.
10 G. Baumann and P. Mueller, *J. Supramol. Struct.*, 1974, **2**, 538–557.
11 K. He, S. J. Ludtke, D. L. Worcester and H. W. Huang, *Biophys. J.*, 1996, **70**, 2659–2666.
12 Y. Pouny, D. Rapaport, A. Mor, P. Nicolas and Y. Shai, *Biochemistry*, 1992, **31**, 12416–12423.
13 S. J. Ludtke, K. He, W. T. Heller, T. A. Harroun, L. Yang and H. W. Huang, *Biochemistry*, 1996, **35**, 13723–13728.
14 K. Matsuzaki, O. Murase, N. Fujii and K. Miyajima, *Biochemistry*, 1996, **35**, 11361–11368.
15 V. N. Kokryakov, S. S. Harwig, E. A. Panyutich, A. A. Shevchenko, G. M. Aleshina, O. V. Shamova, H. A. Korneva and R. I. Lehrer, *FEBS Lett.*, 1993, **327**, 231–236.
16 X. D. Qu, S. S. L. Harwig, A. Oren, W. M. Shafer and R. I. Lehrer, *Infect. Immun.*, 1996, **64**, 1240–1245.
17 J. Chen, T. J. Falla, H. J. Liu, M. A. Hurst, C. A. Fujii, D. A. Mosca, J. R. Embree, D. J. Loury, P. A. Radel, C. C. Chang, L. Gu and J. C. Fiddes, *Biopolymers*, 2000, **55**, 88–98.
18 R. I. Lehrer, A. Barton and T. Ganz, *J. Immunol. Methods*, 1988, **108**, 153–158.
19 V. I. Ternovsky, Y. Okada and R. Z. Sabirov, *FEBS Lett.*, 2004, **576**, 433–436.
20 L. Yang, T. M. Weiss, R. I. Lehrer and H. W. Huang, *Biophys. J.*, 2000, **79**, 2002–2009.
21 S. Luca, H. Heise and M. Baldus, *Acc. Chem. Res.*, 2003, **36**, 858–865.
22 M. Hong, *Acc. Chem. Res.*, 2006, **39**, 176–183.
23 M. Hong, *J. Phys. Chem. B*, 2007, **111**, 10340–10351.
24 J. J. Buffy, T. Hong, S. Yamaguchi, A. Waring, R. I. Lehrer and M. Hong, *Biophys. J.*, 2003, **85**, 2363–2373.
25 Y. Su, R. Mani and M. Hong, *J. Am. Chem. Soc.*, 2008, **130**, 8856–8864.
26 M. C. Wiener and S. H. White, *Biophys. J.*, 1992, **61**, 434–447.
27 D. Huster, X. L. Yao and M. Hong, *J. Am. Chem. Soc.*, 2002, **124**, 874–883.
28 J. J. Buffy, A. J. Waring, R. I. Lehrer and M. Hong, *Biochemistry*, 2003, **42**, 13725–13734.
29 R. Mani, S. D. Cady, M. Tang, A. J. Waring, R. I. Lehrert and M. Hong, *Proc. Natl. Acad. Sci. U. S. A.*, 2006, **103**, 16242–16247.
30 M. Tang, A. J. Waring and M. Hong, *J. Am. Chem. Soc.*, 2007, **129**, 11438–11446.
31 S. J. Opella and F. M. Marassi, *Chem. Rev.*, 2004, **104**, 3587–3606.
32 J. Wang, J. Denny, C. Tian, S. Kim, Y. Mo, F. Kovacs, Z. Song, K. Nishimura, Z. Gan, R. Fu, J. R. Quine and T. A. Cross, *J. Magn. Reson.*, 2000, **144**, 162–167.
33 R. Mahalakshmi, C. M. Franzin, J. Choi and F. M. Marassi, *Biochim. Biophys. Acta*, 2007, **1768**, 3216–3224.
34 F. M. Marassi, *Biophys. J.*, 2001, **80**, 994–1003.
35 M. Tang, A. J. Waring, R. I. Lehrer and M. Hong, *Biophys. J.*, 2006, **90**, 3616–3624.
36 S. Yamaguchi, T. Hong, A. Waring, R. I. Lehrer and M. Hong, *Biochemistry*, 2002, **41**, 9852–9862.
37 M. Hong and T. Doherty, *Chem. Phys. Lett.*, 2006, **432**, 296–300.
38 S. D. Cady, C. Goodman, C. D. Tatko, W. F. DeGrado and M. Hong, *J. Am. Chem. Soc.*, 2007, **129**, 5719–5729.
39 M. Tang, A. J. Waring, R. L. Lehrer and M. Hong, *Angew. Chem., Int. Ed.*, 2008, **47**, 3202–3205.
40 C. Roumestand, V. Louis, A. Aumelas, G. Grassy, B. Calas and A. Chavanieu, *FEBS Lett.*, 1998, **421**, 263–267.
41 J. J. Buffy, A. J. Waring and M. Hong, *J. Am. Chem. Soc.*, 2005, **127**, 4477–4483.
42 W. Luo and M. Hong, *J. Am. Chem. Soc.*, 2006, **128**, 7242–7251.
43 R. Mani, M. Tang, X. Wu, J. J. Buffy, A. J. Waring, M. A. Sherman and M. Hong, *Biochemistry*, 2006, **45**, 8341–8349.
44 M. Tang, A. J. Waring and M. Hong, *J. Am. Chem. Soc.*, 2005, **127**, 13919–13927.
45 S. H. White and W. C. Wimley, *Annu. Rev. Biophys. Biomol. Struct.*, 1999, **28**, 319–365.
46 W. C. Wimley and S. H. White, *Nat. Struct. Biol.*, 1996, **3**, 842–848.
47 T. Hessa, N. M. Meindl-Beinker, A. Bernsel, H. Kim, Y. Sato, M. Lerch-Bader, I. Nilsson, S. H. White and G. von Heijne, *Nature*, 2007, **450**, 1026–1030.
48 T. Hessa, S. H. White and G. von Heijne, *Science*, 2005, **307**, 1427.
49 J. A. Freites, D. J. Tobias, G. von Heijne and S. H. White, *Proc. Natl. Acad. Sci. U. S. A.*, 2005, **102**, 15059–15064.
50 H. D. Herce and A. E. Garcia, *Proc. Natl. Acad. Sci. U. S. A.*, 2007, **104**, 20805–20810.
51 K. A. Schug and W. Lindner, *Chem. Rev.*, 2005, **105**, 67–114.
52 M. Tang, A. J. Waring and M. Hong, *Biochim. Biophys. Acta*, 2008, DOI: 10.1016/j.bbamem.2008.10.027.
53 T. Doherty, A. J. Waring and M. Hong, *Biochemistry*, 2008, **47**, 1105–1116.
54 S. H. Park, S. Prytulla, A. A. De Angelis, J. M. Brown, H. Kiefer and S. J. Opella, *J. Am. Chem. Soc.*, 2006, **128**, 7402–7403.
55 S. Yamaguchi, D. Huster, A. Waring, R. I. Lehrer, B. F. Tack, W. Kearney and M. Hong, *Biophys. J.*, 2001, **81**, 2203–2214.
56 D. Huster, L. S. Xiao and M. Hong, *Biochemistry*, 2001, **40**, 7662–7674.
57 G. Reuther, K. T. Tan, A. Vogel, C. Nowak, K. Arnold, J. Kuhlmann, H. Waldmann and D. Huster, *J. Am. Chem. Soc.*, 2006, **128**, 13840–13846.
58 M. Tang, A. J. Waring and M. Hong, *ChemBioChem*, 2008, **9**, 1487–1492.
59 R. I. Lehrer and T. Ganz, *Curr. Opin. Immunol.*, 2002, **14**, 96–102.

This journal is © The Royal Society of Chemistry 2009